Journal of Energy Storage 84 (2024) 110803

Contents lists available at ScienceDirect

Journal of Energy Storage

journal homepage: www.elsevier.com/locate/est

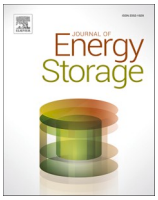

Research papers

Numerical investigation and response surface optimization of a sorption heat storage systems performance using Y-shaped fins

Elham Abohamzeh *, Seyed Ehsan Hosseinizadeh, Georg Frey

Automation and Energy Systems, Saarland University, 66123 Saarbrücken, Germany

ARTICLE INFO

Keywords:
Adsorption
Y-shape fins
Sorption heat storage
Numerical simulation
Optimization
Response surface method

ABSTRACT

Several previously developed prototypes have proven the high energy density of sorption heat storage systems. However, the very poor thermal conductivity of the material bed, especially in closed sorption storage systems, has remained one of the main challenges for introducing this technology to the market. In this paper, the use of straight and Y-shaped fins is investigated to break through the limitation of heat transfer. An axisymmetric transient analysis is established for the adsorption and desorption processes of zeolite/water pair in an adsorption bed containing Y-shaped fins. The results of numerical simulations reveal higher adsorption rates, and improved heat transfer throughout the bed and also between zeolite and heat transfer fluid using Y-shaped fins during the adsorption process, leading to increasing outlet temperature of the heat transfer fluid. The effect of Y-shaped fin length and the angle between the branches has been investigated through a parametric study, aiming to find the optimized fin geometry. The response surface method (RSM) has been applied to relate the achieved outlet temperature to the fin geometry. The investigations were carried out independent of the amount of metal used, to study the improvement only as a result of changing the geometry and arrangement of fins. Based on the investigations, the optimized geometry of the Y-shaped fins has been defined. The average temperature lift for a time period of 800 min has increased by 4.6 K compared to the case with straight fins and 8.7 K compared to the case without fins, and for the average output power, 103 % and 238.8 % improvement is observed compared with the case with straight fins and without fins, respectively. The result of the study for the desorption process shows an increase of 42 K in the temperature of the adsorbent bed for the optimum case compared with the case without fins.

1. Introduction

The building sector constitutes 40 % of global energy consumption. It also contributes 30 % of greenhouse gases yearly [1]. Furthermore, the energy needed for cooling and heating is the highest energy consumption in buildings [2]. With a 1.4 % increase in global energy-related CO_2 emissions, a historic high of 32.5 Gt was observed in 2017 [3]. Considering this, novel technologies like adsorption heating and cooling systems for buildings have attracted a lot of attention, recently. The process in these systems is characterized by a reversible reaction of reactants and products that involves an exothermic synthesis and endothermic decomposition process. The adsorbed and released heat from these reactions can be considered for cooling and heating purposes.

For heating applications, sorption storage systems have been proposed as a solution for storing solar heat in summer and using the stored energy in winter, given the fact that using solar energy is limited considering its variability with location, time, and seasonal availability. Using this storage system, the free solar energy can be stored for periods of low solar irradiation. These systems are considered a promising technology to minimize the temporal mismatch between solar energy supply and heat demand. Compared with other heating storage approaches, latent and sensible, the noticeable advantage of this technology is its long-term energy conservation with high energy density and negligible heat loss. These properties give the process a very advantageous and attractive long-term energy storage at both high and low temperatures [4]. On the other hand, in adsorption cooling systems, the cooling effect is desired and obtained through the reactions between two substances.

The performance of both cooling and heating sorption systems is largely related to the mass and heat transfer inside the adsorbent bed. Considering this, the improvement of these processes has been the subject of several recently conducted studies [5–7]. The focus of these is mostly the materials characterization and reaction kinetics, and the

* Corresponding author.
E-mail address: elham.abohamzeh@aut.uni-saarland.de (E. Abohamzeh).

https://doi.org/10.1016/j.est.2024.110803
Received 17 April 2023; Received in revised form 30 January 2024; Accepted 31 January 2024
Available online 15 February 2024

Nomenclature

C	Water vapor concentration, mol/m^3
C_p	Specific heat capacity, $J/kg{\cdot}K$
E_a	Surface diffusion activation energy, J/mol
h	Heat transfer coefficient, $W/m^2{\cdot}K$
h_{ti}	Heat transfer coefficient between heat transfer fluid and tube, $W/m^2{\cdot}K$
h_{to}	Heat transfer coefficient between heat adsorbent and tube, $W/m^2{\cdot}K$
ΔH	Enthalpy of reaction, kJ/kg
k	Thermal conductivity,$W/m{\cdot}K$
M_w	Average molar mass of water, kg/mol
P	Pressure, pa
R	Universal ideal gas constant, $J/mol{\cdot}K$
T	Temperature,K
u	Water vapor velocity vector, m/s
X	Amount of Adsorbed water vapor per unit mass of the adsorbent, kg_w/kg_s
X_{EQ}	Equilibrium loading, kg_w/kg_s
V	Volume, m^3

Greek symbols

ρ	Density,kg/m^3
ε	Porosity
κ	Permeability, m^2
μ	Viscosity, $kg/m{\cdot}s$

Subscripts

bed	Adsorption bed
co	Copper
con	Condenser
Evap	Evaporator
eff	Effective
EQ	Equilibrium
f	Water vapor
htf	Heat transfer fluid
opt	Optimized
p	Particle
s	Adsorbent, zeolite
sf	Straight fin
sat	Saturation
w	Without fin

improvement of thermal conductivity of sorption materials. A 2D model of an adsorption cooling system has been developed by Çağlar [8] to compare the performance with the finned and finless tube-type adsorbent bed using a water/silica gel pair. A considerable improvement in the adsorbent bed temperature has been observed using the finned tube-type adsorbent bed. Mitra et al. [9] studied the effect of the aspect ratio of the heat exchanger as well as the size of adsorbent particles size on the characteristics of the adsorption process. They have considered two different particle sizes and evaluated three domains of heat exchanges. The domains had various aspect ratios but the same area. Based on the results from their CFD study, the dynamic uptake is strongly dependent on the porous media flow resistance for smaller particle sizes, while a weak dependence was observed on thermal and intraparticle diffusion for particles with larger sizes. Some other studies have focused on optimizing the adsorbent bed for sorption systems. Kant et al. [10] developed a numerical model to investigate the silica gel/water adsorption process in the adsorbent bed containing cylindrical as well as rectangular fins for sorption heat storage purposes. They also conducted a parametric study on fin parameters. The results of their work showed better performance of the rectangular fin compared with the cylindrical one. Golparvar et al. [11] studied the influence of spacing of the fins in a gas-driven adsorption cooling system. Based on their results, higher temperature gradients have been observed for a bed with larger fin spacings, leading to non-uniform desorption and adsorption processes, so decreasing the performance of the adsorption cooling system. Kant and Pitchumani [12] conducted a numerical investigation to investigate the influence of fin tree structure on improving heat transfer in a thermochemical heat storage bed. They optimized the geometry of the fin for maximizing energy storage density and minimize the levelized cost. Reichl et al. [13] investigated two approaches for numerically characterizing adsorption reactors in open sorption systems. The mixing behavior of a rotating drum configuration is assessed using discrete particle models and particle simulations. The CFD simulations revealed enhanced reactor performance by improving particle mixing and reducing temperature differentials. Kurniawan and Rachmat [14] developed a new design for an adsorption chiller with silica gel/water pair, incorporating two sorption chambers with compact fin tube heat exchangers, and conducted a CFD simulation. Based on the results, the outer surface of the adsorbent bed exhibited the highest absolute adsorption rate, while the center displayed the lowest rate. Upon completion of the adsorption process, this trend was reversed, with the center exhibiting the highest and the outer surface showing the lowest rate. Crespo et al. [15] conducted a study aimed to optimize the discharging process of a thermal energy storage system for residential use. The researchers discovered that employing conservative and consistent discharging temperature set points resulted in a 9 % increase in the energy density, as it experienced fewer interruptions during discharge. Additionally, the study explored the influence of weather conditions and various low-temperature heat sources. Overall, the study concluded that an energy density of 139 kWh/m^3 can be achieved with a storage system comprising 20 modules of LiCl-silica gel when a constant low-temperature heat source, such as waste energy or geothermal, was available.

Mohammad et al. [16] performed a numerical and experimental study on an adsorption cooling systems performance and proposed a modular packed bed. Their design showed 2.3 times greater specific cooling power compared to typical adsorption chillers. Considering the advantages of this technology, research in the field of sorption storage has experienced rapid development, in recent years [17]. There is an increasing number of research teams in engineering, chemical, and materials sciences who concentrate on developing this technology [18]. Regarding the materials used for the sorption process, several studies have been conducted in recent years [19,20]. The two most commonly used traditional physical sorbents are silica gel and zeolite. Silica gel is a widely and commercially used, cheap and non-toxic. However, the storage capacity in practice is significantly lower than was theoretically predicted and the sorption heat is also too low, as shown by Jaehnig et al. [21]. Zeolites consist of aluminum silicate minerals, which have very small porous structures. The pores allow them to absorb water and store it temporarily. In contrast to silica gel, they have a high desorption temperature between 150 °C and 300 °C. Furthermore, zeolite has a higher energy density of 3300–4200 kJ/kg [22]. There are a large number of different types of zeolites. Four species are particularly prevalent in sorption storage. These are Zeolites 4A, 5A, 10X and 13X [23]. Herzog et al. [24] studied binderless molecular sieves and identified A, X, and Y molecular sieves as potential low-temperature storage materials (up to 200 °C). Zeolite A is particularly suitable for higher temperatures because it has high thermal stability. For applications under high pressure in a reactor, for example, when working with condensing water, the Y variants are more suitable than the A and X

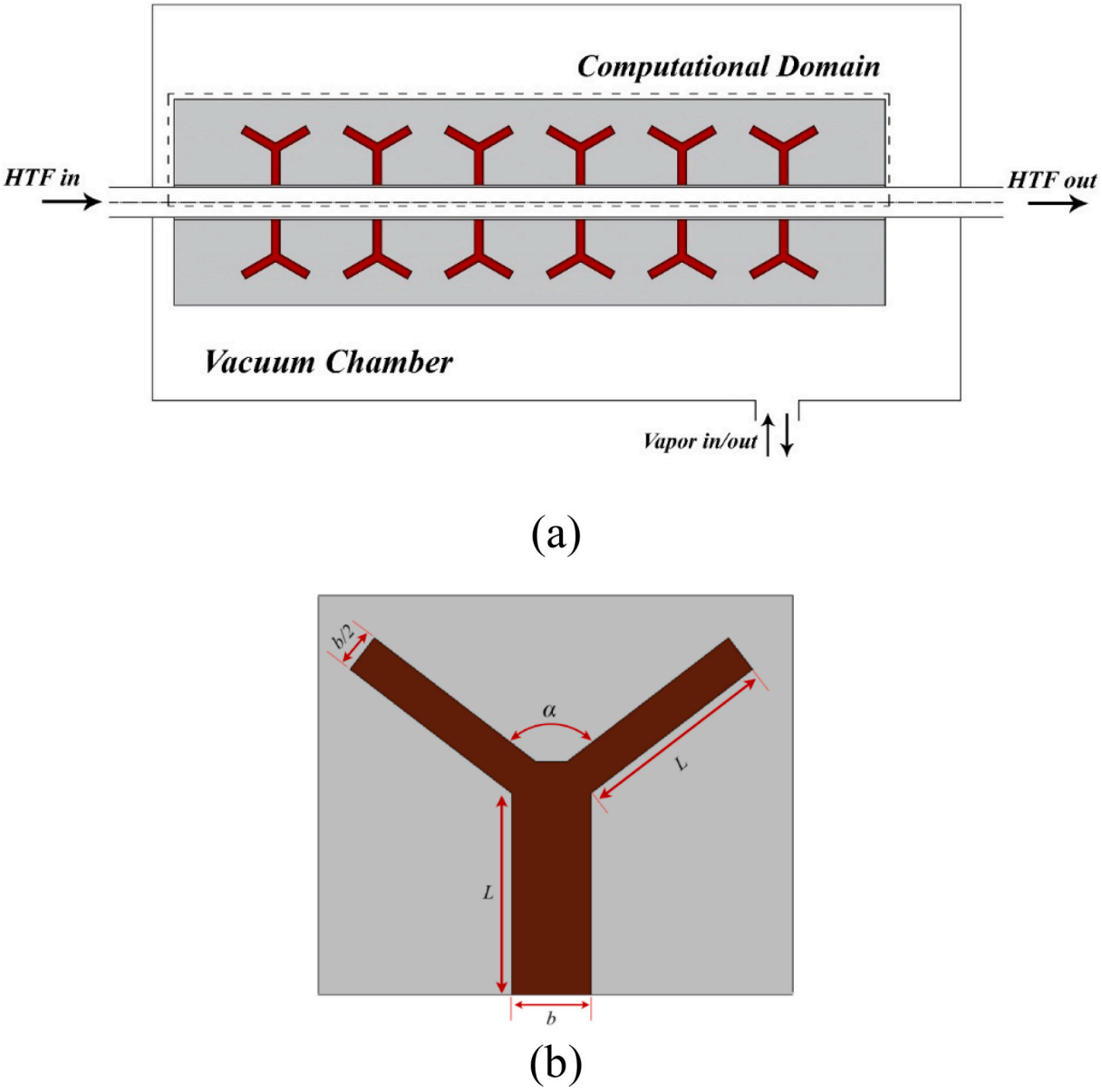

Fig. 1. The schematic showing (a) the adsorbent bed and (b) the geometry of the Y-shaped fin.

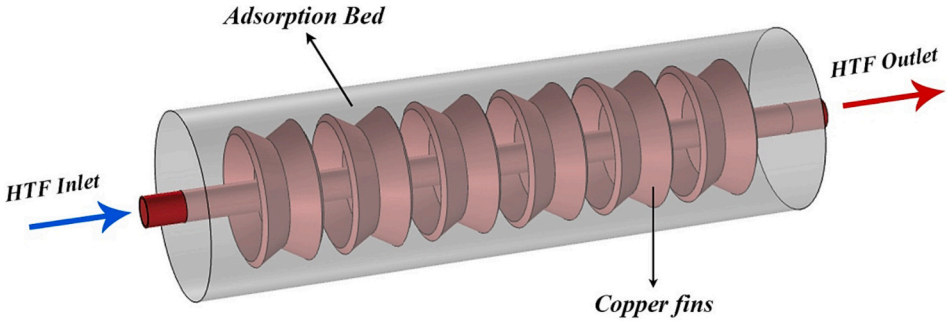

Fig. 2. A schematic of the computational domain

variants. Type X, on the other hand, has better kinetic properties. Type A produces the most usable temperatures.

In this work, the response surface methodology (RSM) is used for optimizing the fin geometry. A series of statistical and mathematical techniques are collected in RSM for optimization purposes. RSM was initially developed for modeling experimental results and after that used to model numerical experiments. Inaccuracy in physical experiments can occur from errors in measurements, but numerical inaccuracy can be

Table 1
Geometrical parameters of the system

Parameter	Value	Unit	Description
L_{bed}	300	mm	Length of the bed
r_o	58	mm	Outer Radii of the bed
r_i	7	mm	Inner Radii of the bed
t	1	mm	Tube thickness
L	10–20	mm	Length of fin
b	4.45–8.6	mm	Thickness of fin
α	0–175	–	Angle between branches

Table 2
Thermophysical properties of the materials

Parameter	Value	Unit	Description
d_p	2	mm	Particle diameter [31]
ε_{bed}	0.37	–	Porosity of desorption bed [32,33]
ε_p	0.42	–	Porosity of zeolite Particle [32,33]
n	1.73	–	Heterogeneity factor
ΔH	3300	kJ/kg	Iso-steric heat of adsorption [31]
R	8.314	J/(mol·K)	Ideal gas constant
M_w	18.02	g/mol	Water vapor molar mass
E_a	10,000	J/mol	Surface diffusion activation energy - zeolite
$k_c k_{co}$	400	W/(m·K)	Thermal conductivity of copper
k_s	0.1	W/(m·K)	Thermal conductivity of zeolite
$\rho_{c\,co}$	8700	kg/m^3	Density of copper
ρ_s	1000	kg/m^3	Zeolite density
$C_{p,c}C_{p,co}$	385	J/(kg·K)	Specific heat of copper
$C_{p,s}$	837	J/(kg·K)	Specific heat of zeolite
$C_{p,htf}$	1930	J/(kg·K)	HTF specific heat
k_{htf}	0.115	W/(m·K)	HTF thermal conductivity
D_0	5.8e−9	m^2/s	Reference diffusivity
$\rho_{p,htf}$	914	kg/m^3	HTF density

Table 3
Considered values for initial and boundary conditions

Parameter	Value	Unit	Description
P_{in}	3	Pa	Initial pressure
T_{evap}	278.15–293.15	K	Evaporator temperature
T_{init}	303.15	K	Initial temperature

due to the discrete representing of a continuous physical phenomenon, round-off error, or incomplete convergence of iterative processes. The use of RSM in the optimization of designs aims to lower the expense of costly analysis techniques (such as CFD analysis or finite element method) and the associated numerical noises [25]. Liu and Yang [26] used RSM to define the impact of different parameters on the performance of concrete thermal energy storage. The results of the study identified the velocity of the heat transfer fluid as the most influential factor for energy efficiency and charging time. Furthermore, the inlet temperature of heat transfer fluid significantly affected energy storage. An optimization process using the desirability function was performed to maximize energy storage efficiency and minimize charging time. Ahmed et al. [27] designed and tested a lab-scale prototype of an innovative concentrated solar-powered flash desalination system. They used RSM for the system modeling and optimizing the developed system and investigated the influence of vacuum pressure, feed water temperature, and flow rate on distillate production. Sun and Zhang [28] proposed a numerical model for predicting the heat transfer and fluid flow on both the water-side and air-side of the elliptical finned-tube heat exchanger. RSM was employed to investigate the influence of seven considered design factors, including the water volumetric flow rate, air velocity, fin pitch, longitudinal and transversal tube pitch, axis ratio, and row number. The findings show that water volumetric flow rate and air velocity strongly interact with the axis ratio. When the water volumetric flow rate is lower or air velocity is higher, increasing the axis ratio improves the thermal-hydraulic performance, whereas the opposite impact is seen at higher water volumetric flow rate or lower air velocity. Alshihmani et al. [29] conducted experiments to investigate the impact of phase change material (PCM) on a printed circuit board's (PCB) performance. The cooling effects of two different PCM types, RT42 and RT35/CH, with various melting points and latent heat of fusion, are compared under both free and forced convection. The study conducts experiments at two heat fluxes and utilizes the response surface method (RSM) to develop predictive models for cooling performance. The results show that using PCM improves module usage time and enhancement ratio, particularly at low heat flux. Increasing PCM volume fraction enhances usage time, with RT42 performing better overall. RSM highlights the significant impact of PCM volume fraction on cooling performance compared to fan voltage.

Although the systems working based on adsorption and desorption processes seem to be a very attractive option for air conditioning applications in buildings considering their high energy density, the poor thermal conductivity in the bed limits the performance of these systems. The focus of this study is developing a coupled mass and heat mathematical model for the simulation of the ad- and desorption process inside the zeolite bed and improving the process using Y-shaped fins. A parametric study has been performed to investigate the influence of geometric parameters of the fin on the adsorption process. The aim is to define the most efficient design of fins that can overcome the poor thermal conductivity of the zeolite bed. The optimized design has been proposed using the RSM analysis. The system performance during both the desorption and adsorption processes has been investigated.

2. Physical model

In this work, a cylindrical fixed bed reactor is considered as the research object in a closed sorption heat storage system, as depicted in Fig. 1. The working principle of the system during the adsorption process can be explained as follows: the process begins with the evaporation of water. The generated water vapor flows into the bed and is adsorbed in the pores of dry zeolite so that the adsorption energy is released. The released heat is extracted by the heat transfer fluid (HTF) flowing through the heat exchanger and is utilized for space heating and domestic hot water. During desorption, the saturated zeolite is dried by the heat provided by hot HTF flowing into the heat exchanger tube. Consequently, the water is released in the gas form, flowing into the condenser and condensing to the liquid [4,30].

The computational domain including the bed filled with zeolite 13X, the tube containing HTF and fins is presented in Fig. 2. The inner and outer tube radii, r_i and r_o, the length of the heat exchanger, L_{bed}, and the thickness, t, are defined as 7 mm, 58 mm, 300 mm, and 1 mm, respectively. Y-shaped fins made of copper are evenly distributed on the surface. The thermophysical properties of water vapor, fin, zeolite, geometrical, and other parameters are presented in Tables 1, 2, and 3 [31,32].

For the length of the fins a range of 10–20 mm and for the angle between the branches a range of 0–175° has been considered, to provide the opportunity for the investigation in a wide range. The thickness of the fins is calculated based on the selected length so that the volume of the fins remains constant for both straight and Y-shaped fins. Hence, the results are independent of the amount of used metal. It should be also mentioned, that this point is also considered for the straight fin type; the thickness and the length of the straight fin are considered so that the volume of the fin would be the same as Y-shaped fins.

3. Mathematical model

3.1. Adsorption model for zeolite 13X

The linear driving force (LDF) model is utilized for modeling the adsorption rate and solving the adsorbed amount [34].

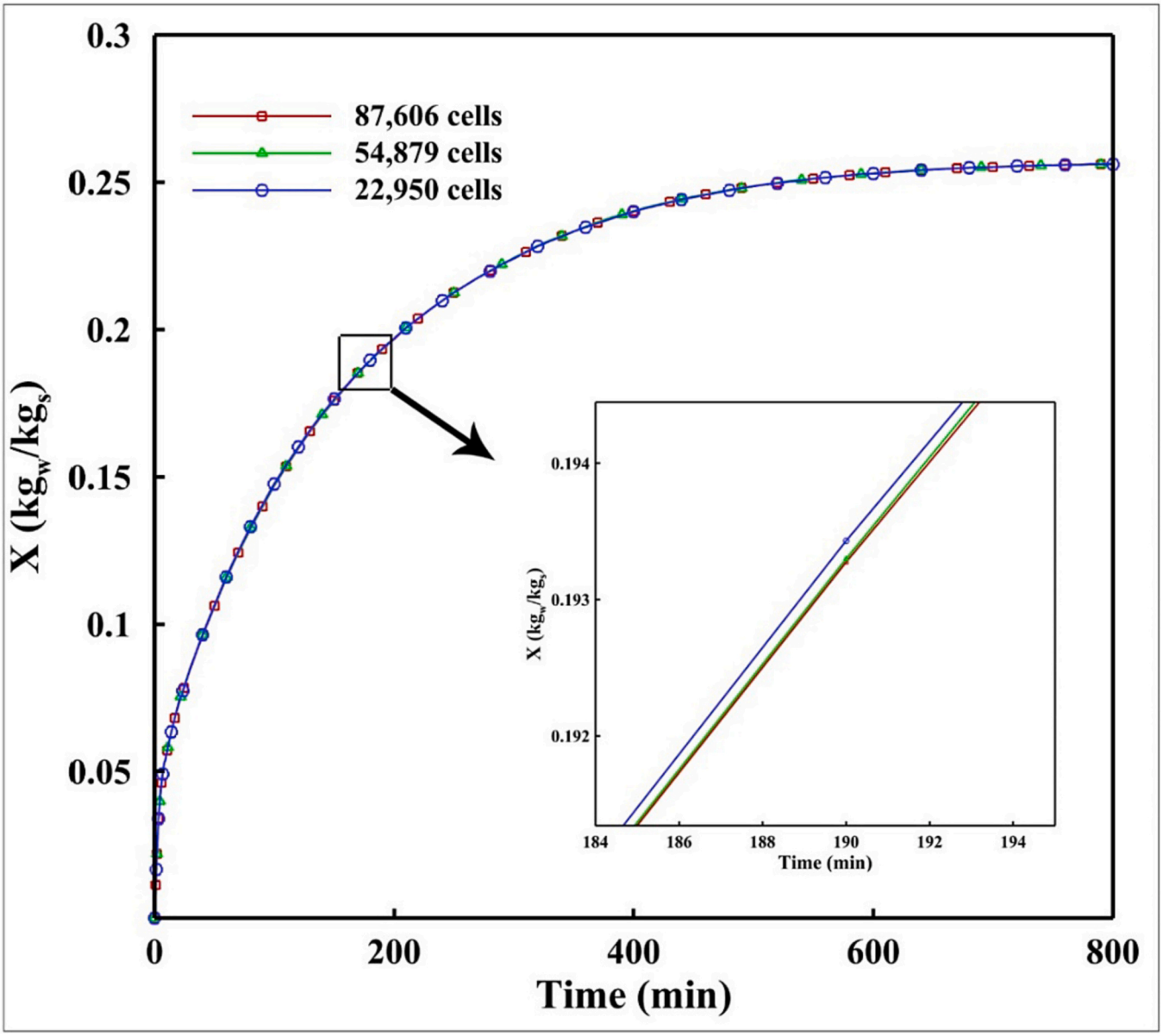

Fig. 3. Grid independence test.

$$\frac{\partial X}{\partial t} = K_{LDF}(X_{EQ} - X) \tag{1}$$

where X_{EQ} is the adsorption capacity in the equilibrium condition and X is the amount of adsorbate that is adsorbed.

K_{LDF} is a lumped mass transfer coefficient, as a measure for defining how easily vapor moves from the adsorbent surface to the particle at the inner points and is defined as [34]:

$$K_{LDF} = \frac{15}{r_p^2} D_o exp\left(-\frac{E_a}{RT}\right) \tag{2}$$

where r_p is the zeolite particle radius, D_o is the reference diffusivity, and E_a represents characteristic energy.

The adsorption equilibrium model is utilized to describe the physical process of water vapor adsorption in the bed and to link between the local circumstances, commonly the temperature and vapor pressure, and the equilibrium water uptake. The model adopted in this study to calculate the equilibrium loading is Dubinin's theory [35]. The basic assumption for using this theory is the pore size which should be <2 nm. This theory says that the adsorbed amount is governed by the micropore volume rather than the surface area of the micropores. The equilibrium water uptake is the theoretical maximum value of the adsorbate which could be adsorbed by an adsorbent bed under specific conditions and can be expressed based on this model as [36,37]:

$$X_{EQ} = X_0 exp\left(-B\left(\frac{T}{T_{sat}} - 1\right)^n\right) \tag{3}$$

where n and B are Dubinin-Astakhov (D-A) fitting coefficients and X_0 is the maximum adsorption capacity for a zeolite 13X-water pair [38].

3.2. Vapor transport in bed

The mass balance equation for the transport of adsorbate gas in the porous domain can be written as [8]:

$$\varepsilon_{eff}\frac{\partial C}{\partial t} - D_{eff}\nabla^2 C + \nabla(C.u) = R_s \tag{4}$$

where D_{eff} is the physical gas diffusivity in the porous domain, C is the

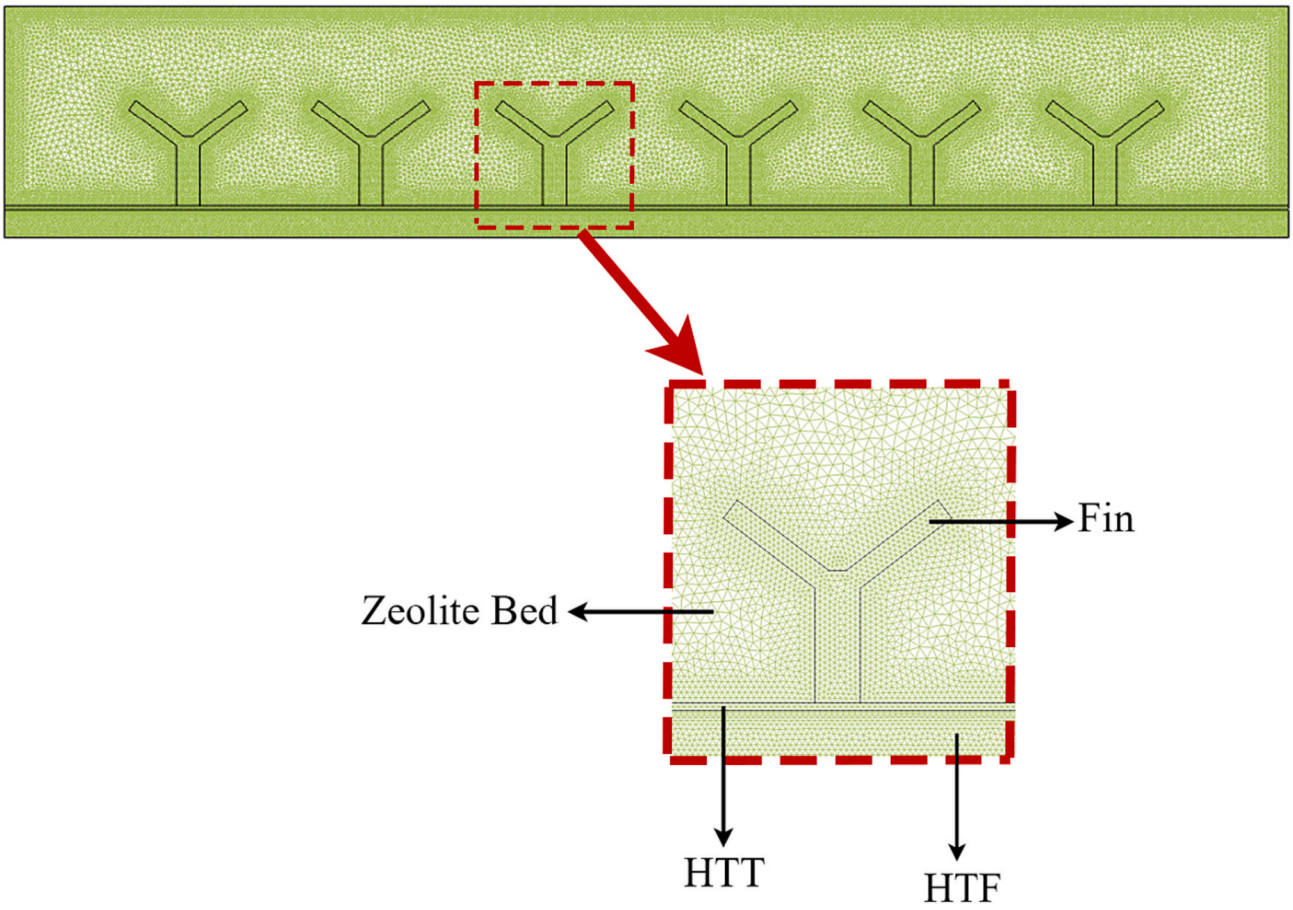

Fig. 4. The quality of computational meshes

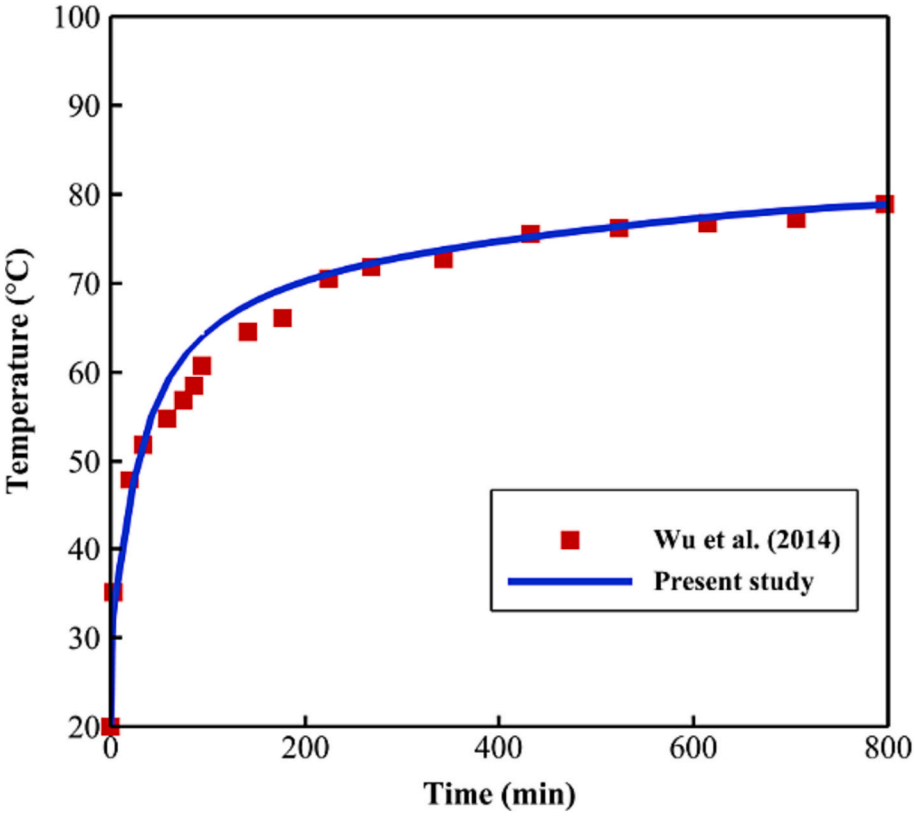

Fig. 5. Validation of the model with the experiments conducted by Wu et al. [48].

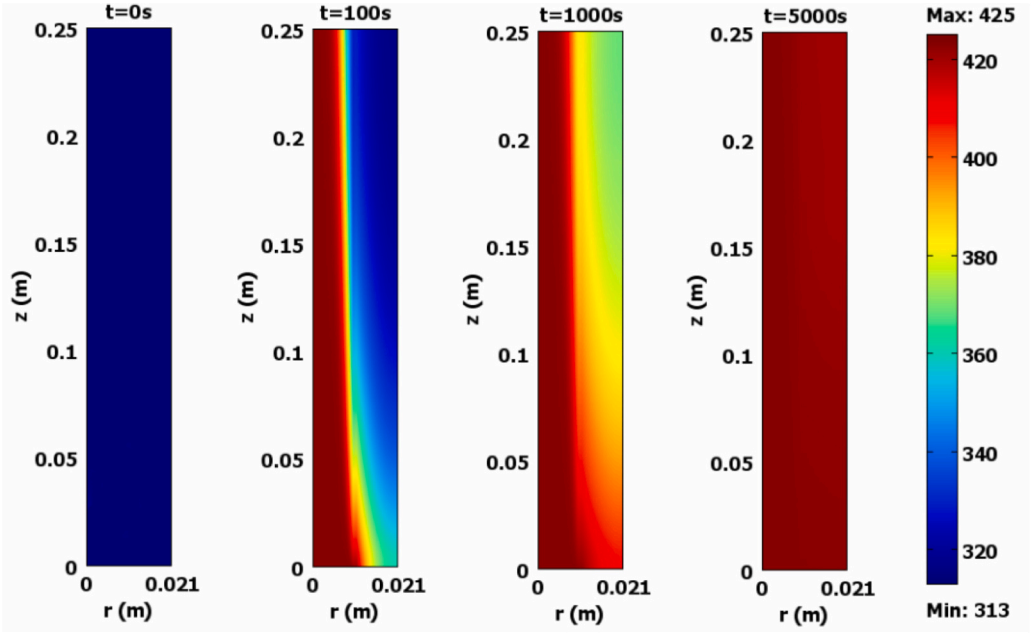

Çağlar. [31]

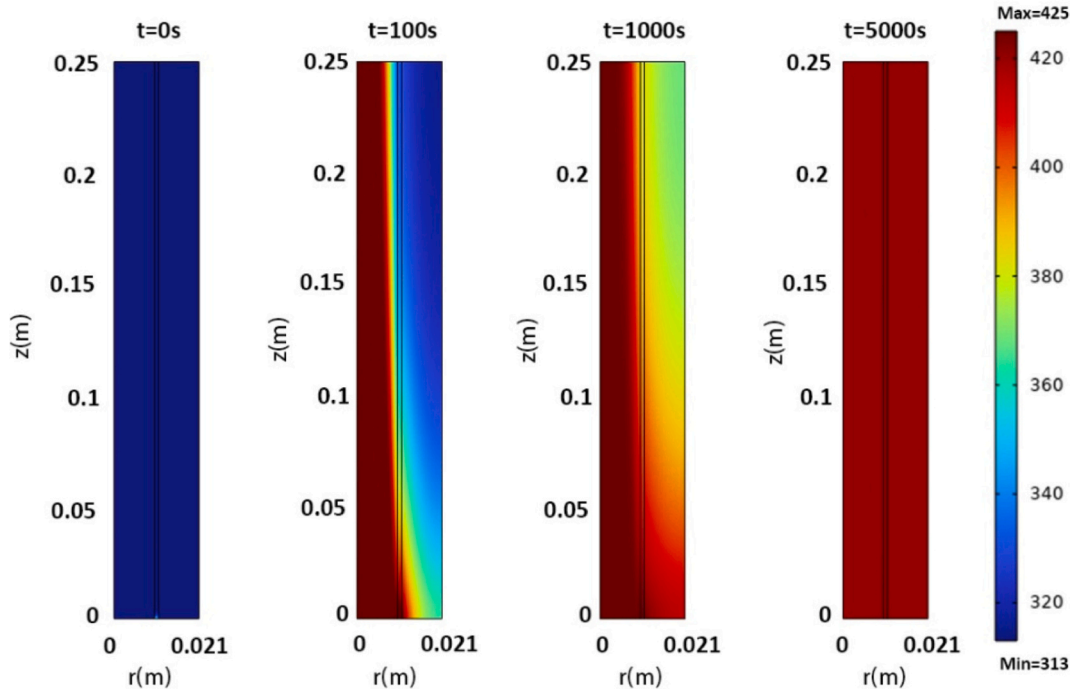

Present Study

Fig. 6. Validation of the model for adsorbent bed temperature with the work of Çağlar [31].

water vapor concentration, ρ_s is the adsorbent density, M_w the water vapor molar mass, and ε_{eff} is the effective porosity and is defined as:

$$\varepsilon_{eff} = \varepsilon_{bed} + \varepsilon_p(1 - \varepsilon_{bed}) \tag{5}$$

where ε_p and ε_{bed} are the particle and bed porosity of zeolite.

In Eq. (4), R_s is the reaction term and can be defined as:

$$R_s = -\frac{(1 - \varepsilon_{eff})\rho_s}{M_w}\frac{\partial X}{\partial t} \tag{6}$$

Under the very low-pressure conditions in this system, the water vapor can be considered as an ideal gas, and the density can be defined based on ideal gas relations, so the pressure, P, of the gas can be given as:

$$P = cRT \tag{7}$$

where T is the temperature and c the water vapor concentration.

The transport of water vapor in the porous media is governed by both diffusion and advection. The pressure difference causes the bulk transport of water vapor. The vapor velocity in axial and radial directions is

Table 4
Design and result of CCD analysis

Case	Fin length (mm)	Corresponding width of the fin (mm)	Angle (°)	Average outlet temperature of HTF (K)
1	15	5.88	175	314.817
2	22	4.1	88	318.462
3	0.8	10.5	88	312.878
4	2	4.45	150	316.651
5	2	4.45	26	317.258
6	1	8.6	26	313.421
7	1	8.6	150	313.366
8	15	5.88	88	315.521
9	12	7.26	45	314.4755
10	15	5.88	0.32	313.852

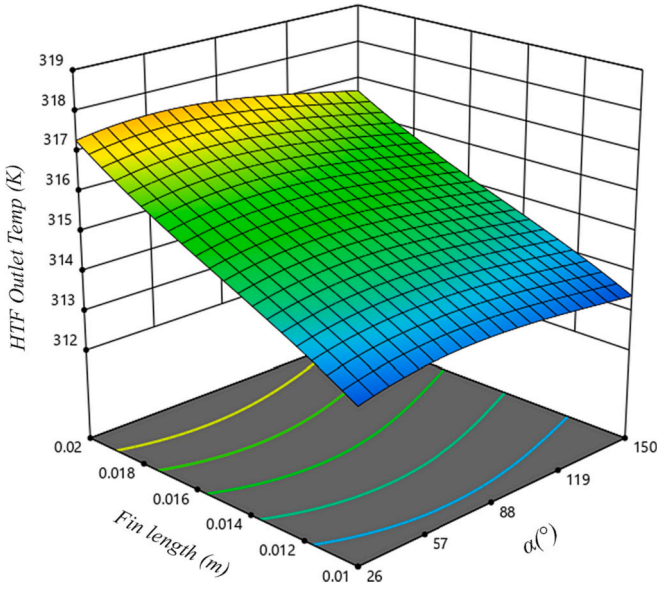

Fig. 7. The change of average temperature of HTF with the length of fin and α.

modeled with the Darcy equation which is valid for the low gas velocities in porous media like the adsorbent bed [10,39]:

$$u = -\frac{\kappa}{\mu}.(\nabla P - \rho_W g) \tag{8}$$

where μ is the gas viscosity, and ρ_W is the gas density. The porous media permeability κ is defined with the semi-empirical Blake-Kozeny equation [40,41]:

$$\kappa = \frac{d_p^2 \varepsilon_{bed}^3}{150\,(1-\varepsilon_{bed})^2} \tag{9}$$

3.3. Heat transfer

Three different domains of adsorbent bed, heat transfer fluid (HTF), fins and heat transfer tube (HTT) are taken into consideration. The heat transfer equations are written for these domains as follows. The governing equation for the porous zeolite is written as [42,43]:

$$(\rho C_p)_{eff}\frac{\partial T_s}{\partial t} + \rho_f C_{pf} u.\nabla T_s - k_{eff}\nabla^2 T_s + \frac{h_{s,co}A_{s,co}}{V_s}(T_s - T_{co}) = Q_s \tag{10}$$

where C_{pf} and ρ_f are specific heat capacity and density of water vapor, and $(\rho C_p)_{eff}$ is the effective volumetric heat capacity and is given by:

$$(\rho C_p)_{eff} = \varepsilon_{eff}\rho_f C_{pf} + (1-\varepsilon_{eff})\rho_s C_{ps} + (1-\varepsilon_{eff})\rho_s C_l X \tag{11}$$

Q_s is the heat generated from adsorbing water vapor in zeolite particles and can be calculated by:

$$Q_s = (1-\varepsilon_{eff})\rho_s \frac{\partial X}{\partial t}|\Delta H| \tag{12}$$

where ΔH is the reaction enthalpy and is given in Table 2.

Heat transfer equation can be considered for heat transfer in fins and heat transfer tube [44,45]:

$$\rho_{co}C_{p,co}\frac{\partial T_{co}}{\partial t} - k_{co}\nabla^2 T_{co} + \frac{h_{ti}A_{ti}}{V_t}(T_{co} - T_{htf}) + \frac{h_{s,co}A_{s,co}}{V_t}(T_{co} - T_s) = 0 \tag{13}$$

where k_{co}, $C_{p,co}$, and ρ_{co} are thermal conductivity, specific heat capacity, and density of the copper fins, respectively.

The governing equation for heat transfer fluid domain includes only convection and conduction and can be written as:

$$\rho_{htf}C_{p,htf}\frac{\partial T_{htf}}{\partial t} + \rho_f C_{p,f}\nabla T_{htf} - k_{htf}\nabla^2 T_{htf} + \frac{2}{r_t}h_{ti}(T_{htf}|_{r=r_t} - T_{co}) = 0 \tag{14}$$

3.4. Definition of Initial and boundary conditions

For the adsorption process, the conditions can be described in the following way:

- An initially uniform distribution is considered for temperature, pressure, and adsorbed amount in the entire domain (porous media, heat transfer fluid, and tube):

  $X = X_i, P = P_i$

$$T_{fin}(t=0) = T_{co}(t=0) = T_s(t=0) = T_{in}$$

$$X_i = X_{eq}(P_i, T_i)$$

$$c_i = \frac{P_i}{RT_i}$$

- A zero temperature gradient is considered at the inlet and outlet of the tube ($\frac{\partial T_f}{\partial z} = 0\ \frac{\partial T_{co}}{\partial z}|_{z=0,L} = 0$)
- Considering the insulation, it can be assumed that the temperature of HTF at the outlet along the axial direction remains constant ($\frac{\partial T_{htf}}{\partial z} = 0$).
- For the bed, a zero temperature gradient is considered at z = 0 and z = L, due to the insulation ($\frac{\partial T_f}{\partial z} = 0$, $\frac{\partial T_s}{\partial z}|_{z=0,L} = 0$).
- The outside boundary of the adsorbent bed is considered adiabatic because of the low vapor pressure and the negligible heat transfer ($\frac{\partial T}{\partial r}|_{r=r_b} = 0$).
- The pressure gradient in the direction normal to the plane is set to zero where the adsorbent boundaries are enclosed by the tube and fins ($\frac{\partial P}{\partial n} = 0$).
- The vapor in the boundaries of the adsorbent bed which are open to the evaporator is at the evaporator pressure ($P|_{r=r_t} = P_{evap}$).

3.5. Response surface methodology

The design optimization applying response surface methodology (RSM) has been used widely in both industry and research, with the aim

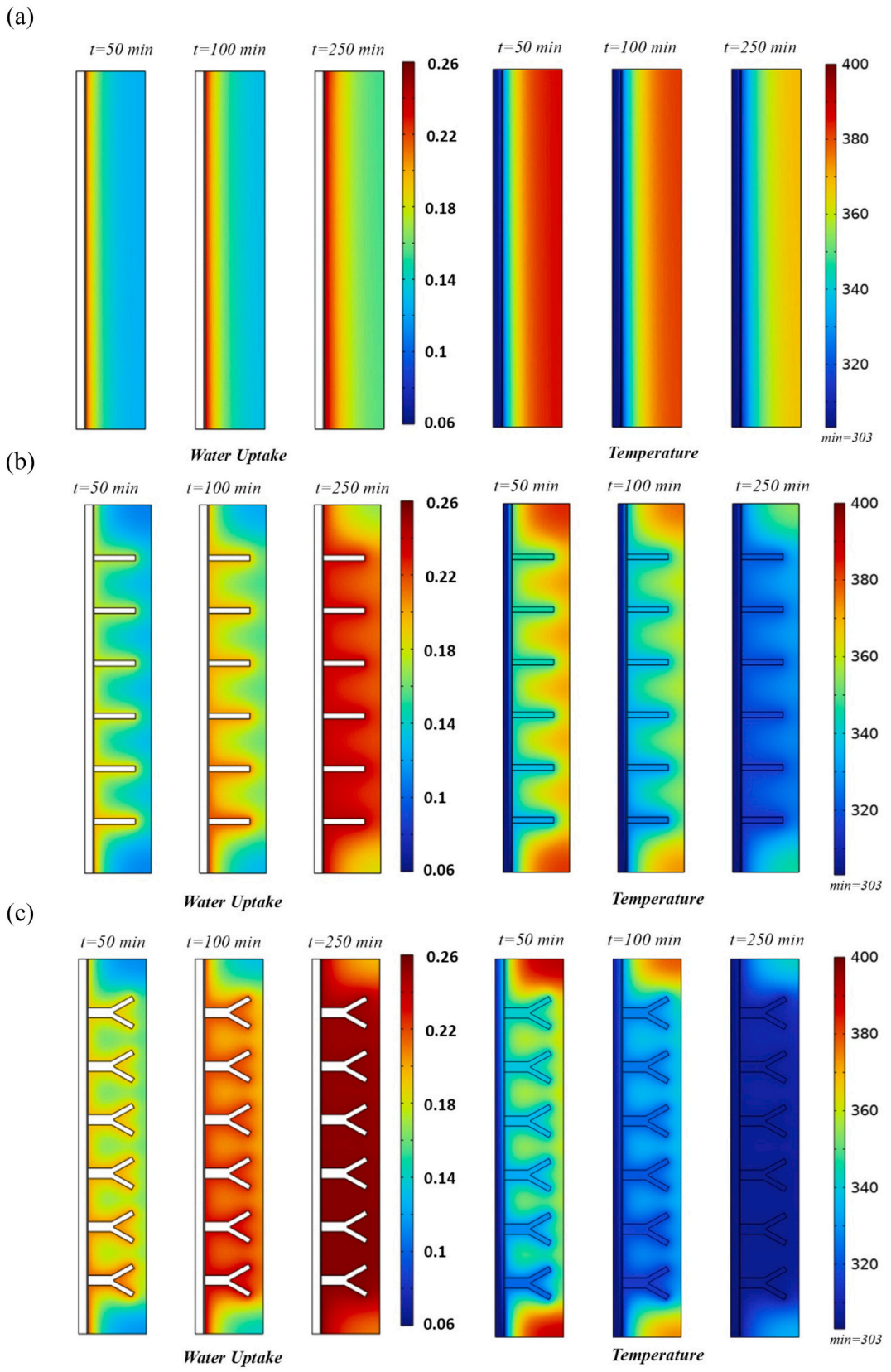

Fig. 8. Variation of temperature and water uptake at 50, 100, and 250 min for cases (a) without fin (b) with straight fin, and (c) with optimized Y-shape fin

of reducing the number of experiments and at the same time, realizing enough data for understanding the influence of under-study parameters on the desired output [46,47]. To better study the effect of branch angle and length of the fins on the adsorption process, the simulation experiment has been conducted according to RSM based on central composite design (CCD) in this study, applying the following steps:

(1) Selection of the response: The purpose of the present study is to reach the highest possible average outlet temperature at the outlet of HTF ($T_{ave,out}$) considering different fin designs.
(2) Choosing variables and assigning codes to them: The parameters which influence the response, are defined. In this study, the fin geometrical parameters, length (L), ranging from 10 to 20 mm, and angle between branches (α), ranging from 0° to 175° are considered for the study.
(3) Experimental design development
(4) Regression analysis
(5) A quadratic polynomial Formation i.e. response development

4. Numerical method

The available finite element method (FEM) based CFD solver, COMSOL Multiphysics 6.1 is utilized to solve the coupled mass and heat transfer equations. User-defined functions are written for programming the reaction kinetics and thermophysical properties expressions. The available interfaces of 'heat-transfer-in-porous-media' and 'transport-of-diluted-species-in-porous-media' are used for programming the equations in COMSOL. The computational grid is generated by discretizing three separated domains of heat transfer fluid (HTF), heat transfer tube (HTT), and adsorbent bed (porous domain) in extremely small elements, aiming to get high precision of the numerical results. The discretization of all equations was done using the quadratic second-order method. Although the maximum time step is considered equal to 1 s, the solver set a very small value for the time step at the initial step of convergence.

4.1. Meshing and grid independence test

To decrease the error of the calculations, a very decreased grid size is considered close to the interfaces of the porous medium and solid. The grid-independent study is conducted on the case with the fin length of 0.015 m and the angle between branches of 105° to confirm that the obtained solutions are independent of the grid resolution. Three different grid sizes of 22,950, 54,879, and 87,606 triangular elements are considered for simulations, and obtained water loading amounts were compared. The results obtained for a very fine mesh with 87,606 elements did not exceed 0.02 % of the results of the case with 54,879 elements. The independent verification of the grid is shown in Fig. 3. Finally, the mesh with 54,879 elements was used for calculation. The mesh quality is depicted in Fig. 4. The minimum and maximum element size of the used grid is 0.0000232 m and 0.00162 m, respectively, so the grid is sufficiently dense to get solutions that are accurate and independent from the mesh size.

4.2. Validation

To confirm the accuracy of the current simulation, the model was validated through the comparison with the results of previous experimental works and also numerical simulations in the literature. The developed model has been validated for the desorption process in a closed system with experiments of Wu et al. [48], on a system including a cylindrical silica gel bed and a water jacket around the bed, acting as a heat source. The cylindrical bed had inner and outer radii of 0.01 and

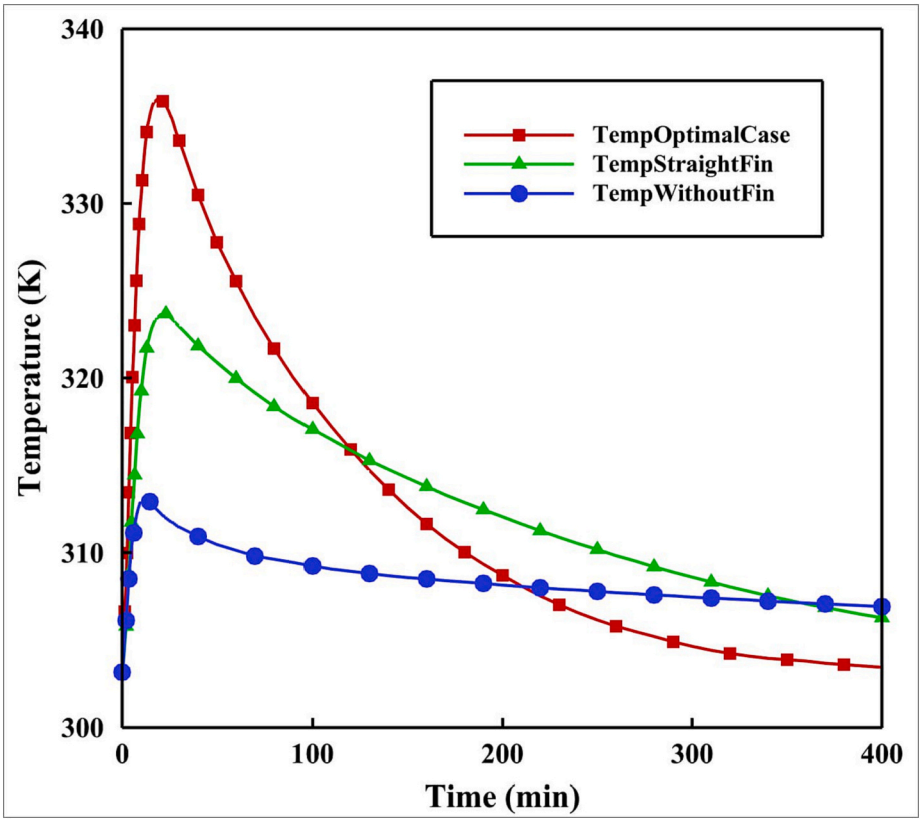

Fig. 9. The effect of the fin type on the outlet temperature of HTF

0.11 m, respectively. The heat exchange with the bed is through the hot water flows by a water jacket. A condenser with a pressure of 2337 Pa is connected to the inner surface of the silica gel. The initial temperature and pressure were 20 °C and 1000 Pa, respectively. The temperature of the cooling and heating water was 20 °C and 80 °C, respectively. Silica gel is dehydrated through the transportation of heat in the bed and thermal energy is stored. The results of the simulation have been compared with the data from experiments considering the temperature at the radius of 100 mm, as shown in Fig. 5.

Further, the numerical model has been also validated with the study by Çağlar [31] on a closed sorption system. The results are presented in Fig. 6.

As can be observed in Figs. 5 and 6, there is a good agreement between the results from the present developed model and that from literature, showing the accuracy of the developed model for further numerical calculations.

5. Results and discussion

To study the effect of using Y-shaped fins on the performance of the system, numerical investigations have been performed. Several simulations have been conducted to evaluate the effect of fin length and the angle between branches on the system performance. Based on the obtained results, the optimal geometry has been proposed for the considered parameters range. Moreover, the influence of fin length and numbers, fin type, and angle between branches and evaporator pressure on the adsorption process has been investigated and evaluated considering the water uptake of zeolite, bed temperature, outlet temperature of HTF, and power output. The power output has been defined as the energy transferred to the HTF per unit of surface area and unit of time. Further, the performance of the optimized case has been compared with the case with a straight fin and without fin for both the adsorption and desorption processes.

5.1. RSM optimization of the geometry

The influence of fin length and the angle between branches on the performance of the system has been studied utilizing RSM. With considering these two parameters as independent variables and the average outlet temperature of HTF as evaluation index, simulations have been conducted. The results of conducted simulations are shown in Table 4. It should be mentioned that the pressure of 3 Pa and the initial temperature of 30 °C are taken for all cases. The evaporator temperature is considered to be 15 °C, which corresponds to a pressure of 2334 Pa.

According to the data in Table 4, the obtained equation for the average outlet temperature of HTF from CCD analysis is:

$$T_{out\_ave} = 309.191 + 348.6953(L) + 0.02186(\alpha) - 0.445231(L\alpha) + 2199.6403(L^2) - 9.4394(\alpha^2) \quad (15)$$

where $0^\circ < \alpha < 175^\circ$, $10\ (mm) < L < 20\ (mm)$. The influence of these parameters on the HTF outlet temperature, based on RSM is presented in Fig. 7. As can be observed, there is a direct relationship between the length of the fin and the outlet temperature. That also shows the importance of the length compared to the width of the used fin, since the longer length corresponds to a smaller width. On the other hand, with increasing α, first, the outlet temperature increases but then decreases. Based on RSM analysis, When the angle is 58° and the length is 0.02 m, the outlet temperature reaches its maximum, 317.5 K.

5.2. The influence of the fin type

Three different cases have been considered for investigations: without fin (C_w), with straight fins (C_{sf}) and with optimized Y-shaped fins (C_{opt}). The variation of temperature and water uptake for different cases is depicted in Fig. 8. As can be observed, the temperature is lower around the fins, and the amount of water uptake increases in these areas. It can be explained by better heat exchange between the cold HTF and bed, so the bed temperature decreases significantly in these areas, and based on Dubinin-Astakhov-formula, Eq. (3), decreasing the adsorption bed temperature leads to augmenting the adsorption capacity of zeolite, so a higher amount of water can be adsorbed. On the other hand, enhanced heat generation and better heat transfer resulting from optimum fin design lead to reaching higher outlet temperatures for HTF, which is the most important objective in heat storage systems. The outputs of the numerical investigation for the outlet temperature of HTF for C_w, C_{sf} and C_{opt} are given in Fig. 9, which shows that the outlet temperature of HTF increases significantly using optimized Y-shaped fins. Average temperature lift of HTF for C_w, C_{sf} and C_{opt} is 5.95, 9.92, and 14.5 K, respectively, showing a 46 % improvement for the optimized case compared with the case with straight fins, and 143.5 % compared with the case without fins. An enhanced heat transfer in the optimized case leads to not only higher energy transfer to HTF from the zeolite area but also decreases the bed temperature and augments the adsorption rate, which in turn augments the heat generation in the adsorption

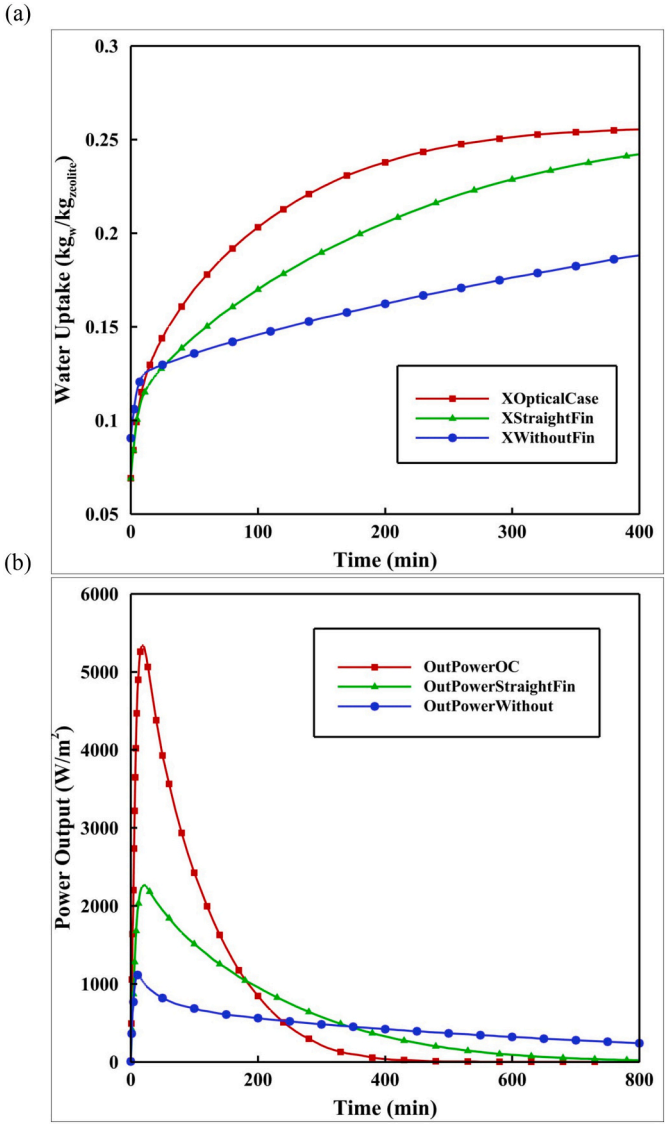

Fig. 10. Variation of (a) water uptake and (b) output power for the case without fin, with straight fin, and with Y-shaped fin

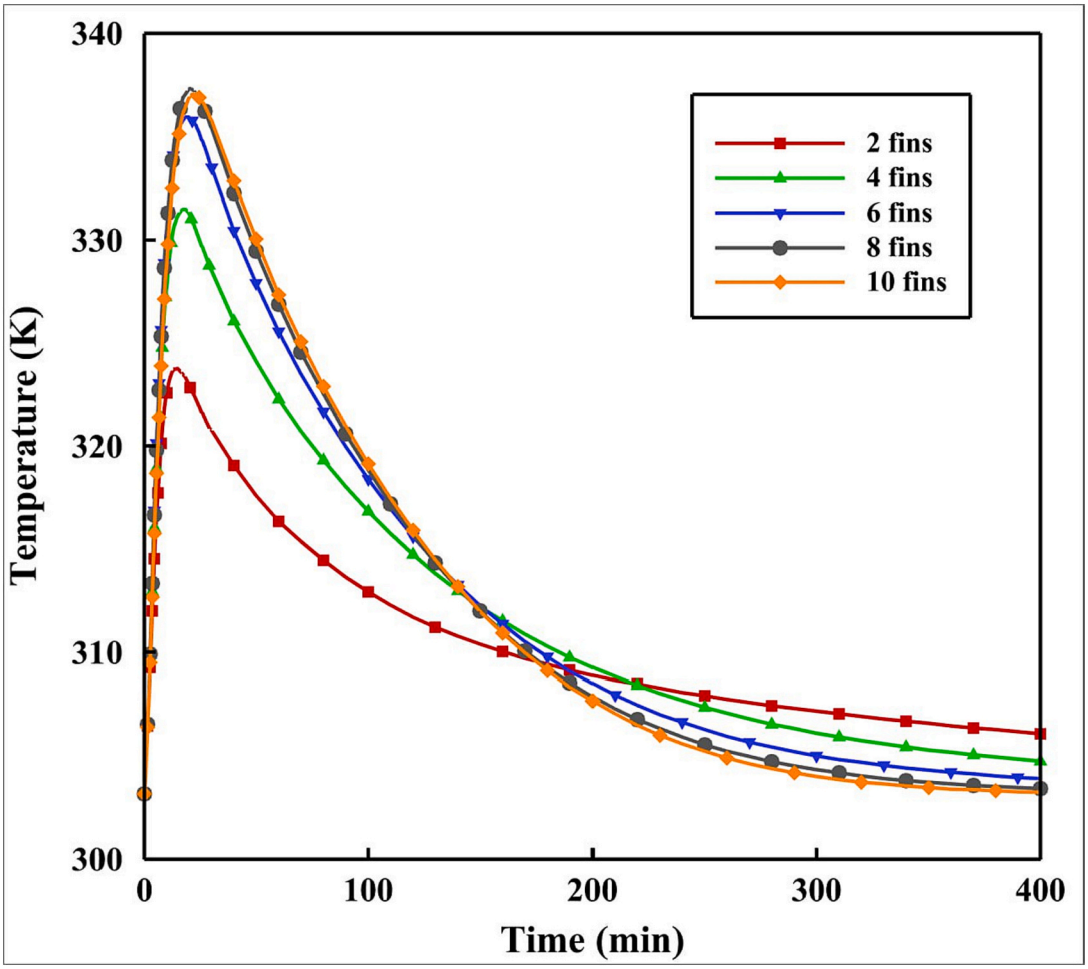

Fig. 11. The effect of fin numbers on average outlet temperature of HTF.

process, reaching higher outlet temperature in HTF area.

The amount of adsorbed water and output power at the tube surface in contact with HTF for the cases of C_w, C_{sf}, and C_{opt} is presented in Fig. 10. The equilibrium uptake is much higher than the actual amount of adsorbate in the bed at the beginning of the process, so based on the LDF model, Eq. (14), the water uptake is high, leading to very high output power. The sharp increase in output power can be also explained by this model. Over time and with adsorbing water, the difference between the equilibrium loading and actual uptake reduces, leading to decreasing the adsorption rate of water. The higher amount of power output in C_{opt}, Fig. 10b, is due to the higher amount of adsorbed water by the adsorbent bed. The average amount of output power in the time period of 800 min for cases of C_w, C_{sf}, and C_{opt} is 668.6 W/m^2, 1115.7 W/m^2, and 2265.4 W/m^2, respectively.

5.3. The effect of fin numbers

To evaluate the influence of fin numbers on the performance of the system, different fin numbers of 2, 4, 6, 8, and 10 have been considered. The length, width and angle, and boundary conditions for all cases are the same as in the optimal case defined based on RSM analysis. The results of an investigation on the temperature, water uptake, and output power at different time intervals are presented in Figs. 11 and 12. It can be clearly observed in Fig. 10, that with increasing fin numbers, the water uptake and average outlet temperature of HTF increase. More fins provide more heat transfer areas between the adsorption bed and HTF area, leading to more efficient heat transfer. So the heat generated from the adsorption process can be better absorbed by HTF and the bed temperature decreases, causing higher adsorption capacity and heat generation in the zeolite bed, leading to higher output power.

The effect of fin numbers on changes in temperature as well as adsorbed water with time is illustrated in Fig. 13. The better heat exchange and higher water uptake with increasing fin numbers lead to a considerable increase in output power, as illustrated in Fig. 12.

5.4. The influence of the length and branch angles of fins

The numerical investigations have been performed for different fin lengths between 0.01 and 0.02 m. It should be noted, that since the volume of the fins is kept constant for all cases, the fins with a longer length have shorter widths. According to the outputs of simulations as well as the RSM analysis, the length of the fin has the most considerable effect on the system performance. With increasing the fin length, the heat exchange between the bed improves, leading to a higher outlet temperature of HTF. At the same time, better heat exchange causes decreasing the bed temperature through the adsorption process, leading to augmenting the adsorption capacity of zeolite. As a result, the amount of adsorbed water and the adsorption rate of the process increases, which also increases the heat generation in the process.

The angle between two branches of the fin is referred to as the branch

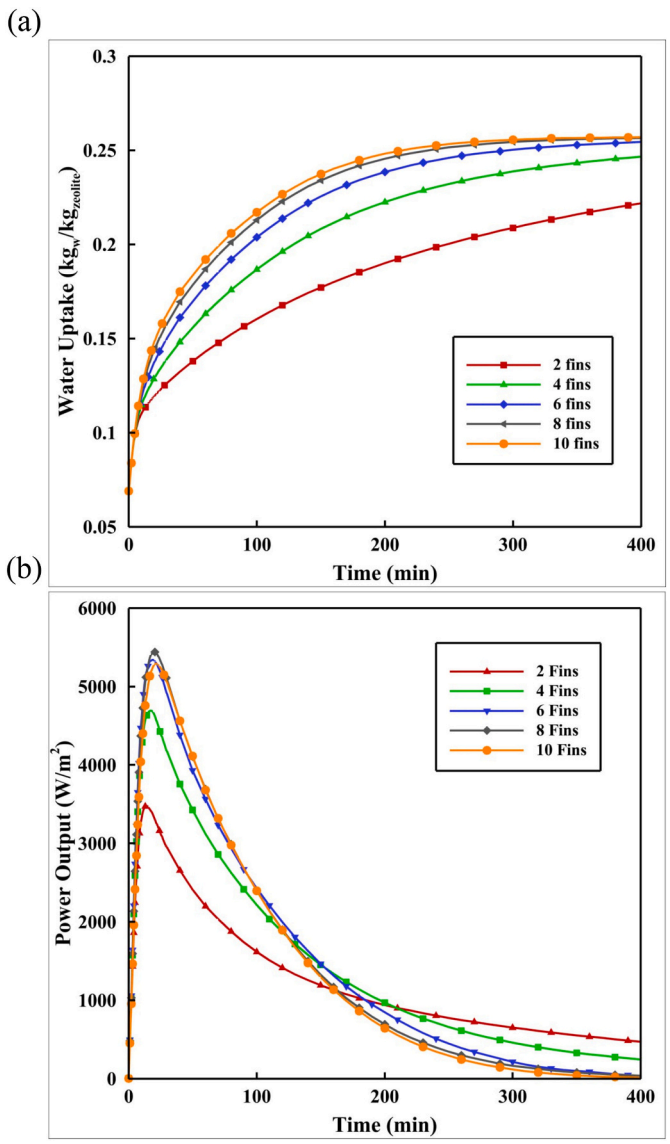

Fig. 12. The effect of fin numbers on (a) water uptake and (b) output power.

angle. With increasing this angle from 0° at the constant length of the fin, the heat transfer process improves, because there is more contact area between the bed and fin, until an optimized angle. After this point, the performance decreases, which can be explained by considering the fact that the water vapor cannot easily penetrate into the areas under the secondary branch, which can negatively affect the adsorption process. However, the influence of the branch angle on the adsorption process here is not too strong. The temperature and water uptake contours and also output power for three different cases with the same fin length of 15 mm but different branch angles of 10, 58, and 175° are presented in Figs. 14 and 15.

5.5. The influence of pressure in the evaporator

One important factor influencing the efficiency of the adsorption process, and so the reachable outlet temperature is the concentration of incoming water vapor flowing from the evaporator into the reactor. The concentration depends on the saturation pressure of the water vapor flow, which itself depends on the temperature of the evaporator. To determine to which degree the storage system performance is influenced by this pressure, simulations are performed for three different evaporator temperatures of 278.15 K, 283.15 K, 293.15 K, and 298.15 K corresponding to the pressure of 837, 1230, 2334, and 3176 Pa. The influence of this pressure on outlet temperature variations and water uptake is presented in Fig. 16. Based on the results, the amount of water uptake increases with increasing the evaporator pressure, leading to a greater temperature in the adsorption bed, and outlet temperature of HTF, as can be observed in Fig. 17. This can be explained based on the reaction kinetics. The adsorption potential increases with the increase of evaporator pressure, leading to augmenting water vapor adsorption rate and increasing bed temperature. Dubinin-Astakhov (D–A) equation says that by increasing the pressure of adsorbate and decreasing the temperature of adsorbent, the adsorption capacity of zeolite augments.

5.6. The influence of the optimum design on the desorption process and the efficiency of the reactor

In order to study the effect of adding fins to the bed on the desorption process, simulations were performed for two cases without fins and with Y-shaped fins (optimum case). The parameters used for developing the numerical model of the desorption process are given in Table 5.

Considering the boundary conditions, the vapor in the boundaries of the bed which are open to the condenser is considered at the condenser pressure ($P|_{r=r_t} = P_{Con}$) and $X(t=0,r,z) = X_0 = 0.26$. The rest of the initial and operating conditions and characteristics are considered the same as for the adsorption process.

The results of the simulation in terms of the average temperature of the adsorbent bed over time are reported in Fig. 18. As can be observed, the average temperature of the zeolite bed has been significantly increased using the optimum shape of Y-shaped fins, resulting in improved performance of the desorption process. The average temperature for the time period of 800 min is 396 K and 354 K for the optimum case and the case without fins, respectively.

5.7. The influence of the optimum design on the efficiency of the reactor

The desorption process involves the release or removal of the adsorbate molecules from the sorbent structure and is an endothermic reaction. During this process, the heat is stored in the zeolite bed due to the thermochemical dissociation between water and zeolite. It can be achieved by applying heat from an external heat source. A part of provided heat is stored in the form of chemical energy. The efficiency of this process can be defined as the enthalpy change during the desorption reaction divided by the energy provided by HTF:

$$\eta_{Des} = \frac{\left(\iint Q_s dvdt\right)_{Des}}{\int_0^t \dot{m} C_{p,htf}\left(T_{Des,in} - T_{Des,out}\right)dt} \tag{16}$$

where $\dot{m}$ is the mass flow rate of the HTF, $C_{p,htf}$ is the specific heat capacity of the HTF, $T_{Des,\ in}$ and $T_{Des,\ out}$ are the inlet and outlet temperatures of the HTF.

During adsorption, water molecules in the gas phase adhere to the surface of the zeolite material. As a result, the enthalpy of adsorption is released and extracted by the same HTF cycle as in the desorption phase via the reactor heat exchanger. The efficiency of the adsorption process can be quantified by the ratio of the useful energy absorbed by HTF to the heat released during the reaction [49]:

$$\eta_{Ad} = \frac{\int_0^t \dot{m} C_{p,htf}\left(T_{Ad,out} - T_{Ad,in}\right)dt}{\left(\iint Q_s dvdt\right)_{Ad}} \tag{17}$$

$T_{Ad,\ out}$ and $T_{Ad,\ in}$ are the outlet and inlet temperatures of the HTF.

The efficiency of the reactor during the desorption process has been

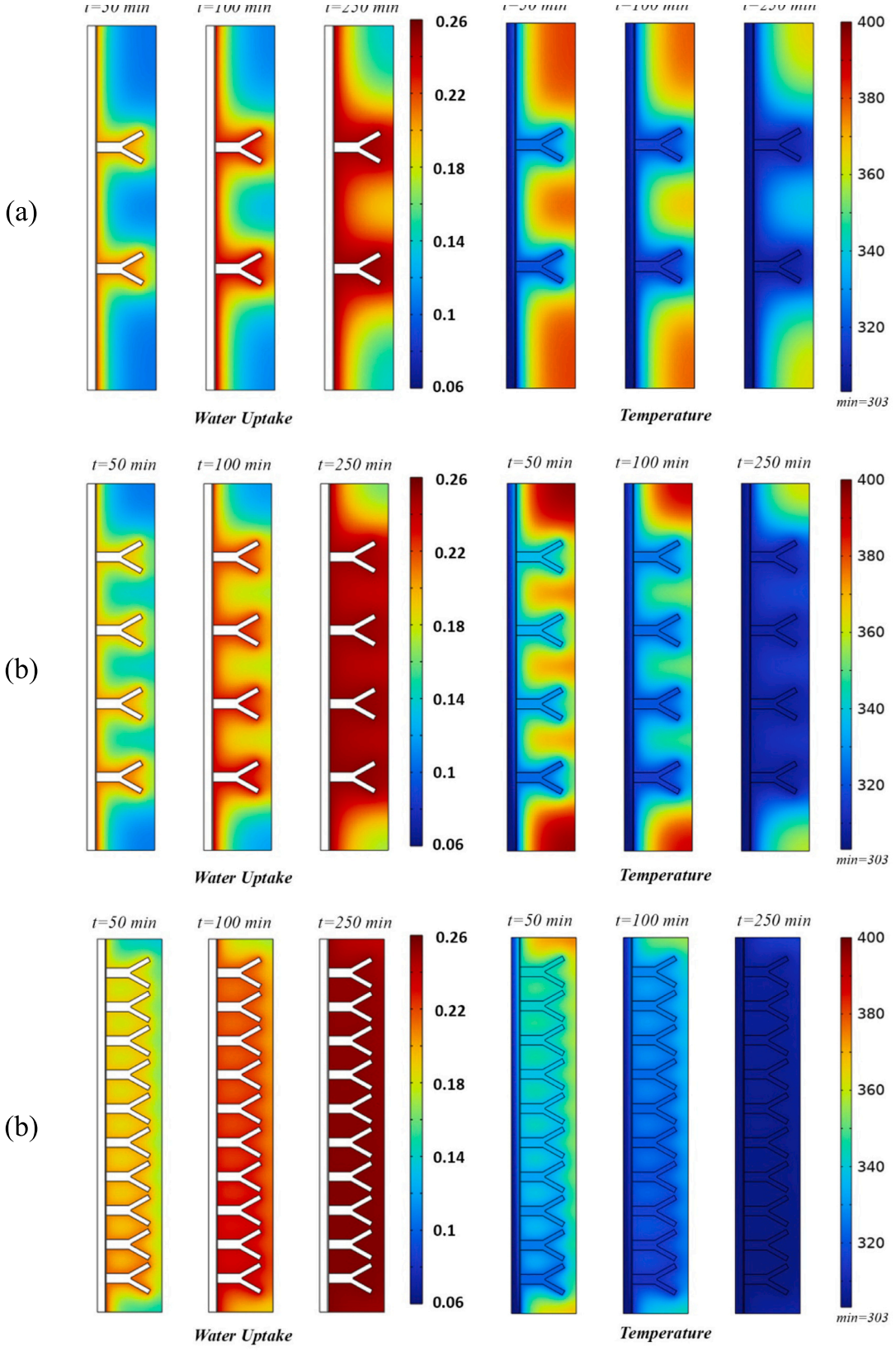

Fig. 13. The effect of fin numbers on the temperature as well as water uptake variations with time for cases (a) with 2 fins, (a) with 4 fins, and (a) with 10 fins

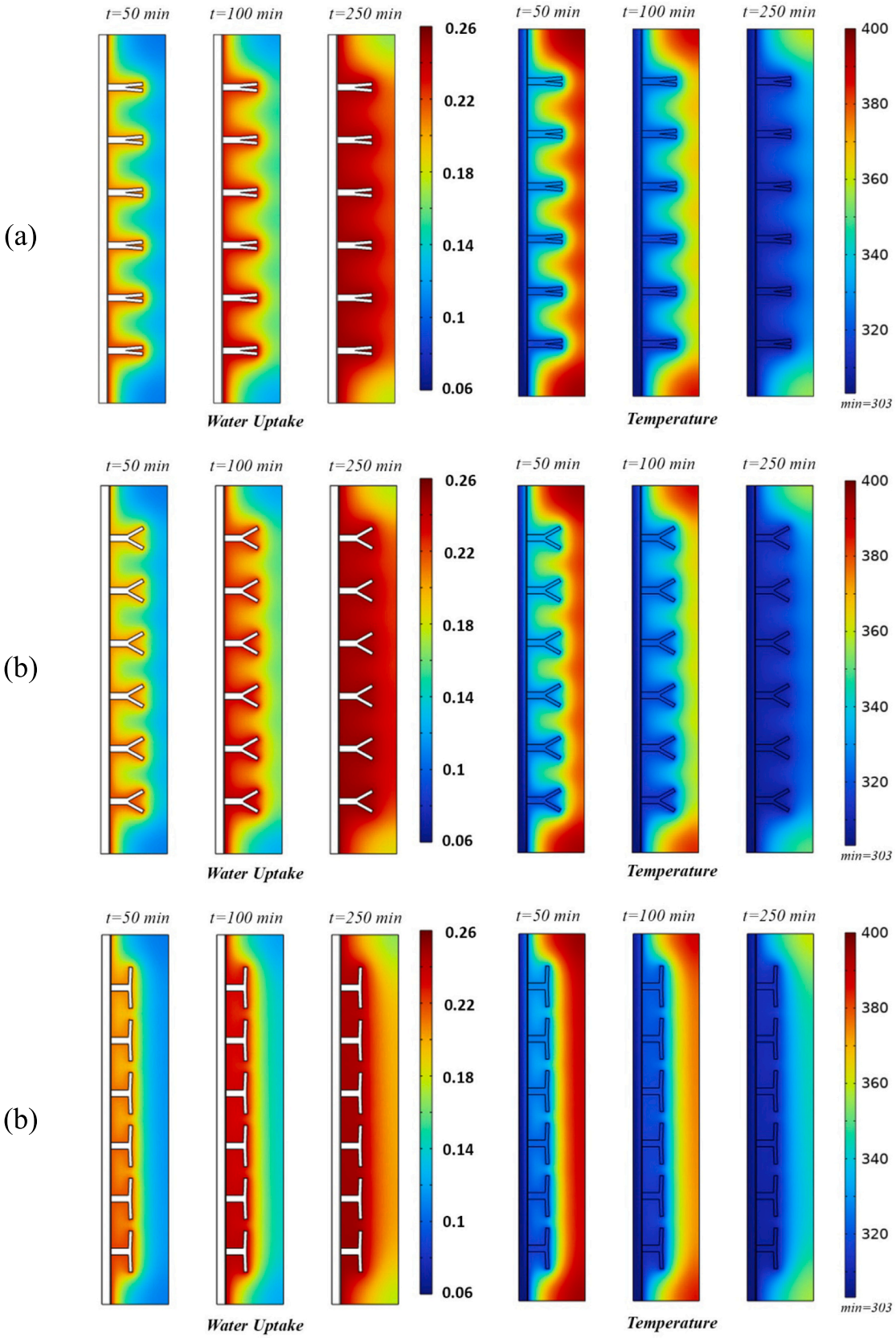

Fig. 14. The effect of the branch angles on the variation of water uptake and temperature with time for cases with Y-shaped fins with (a) L = 15 mm, $\alpha = 10^{\circ}$, (b) L = 15 mm, $\alpha = 58^{\circ}$, and (c) L = 15 mm, $\alpha = 175^{\circ}$

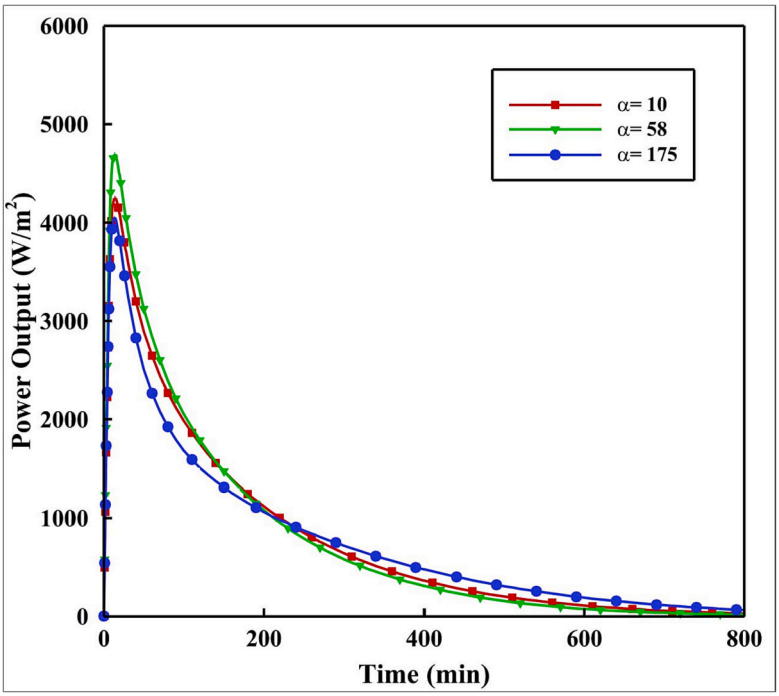

Fig. 15. The influence of branch angle on the output power

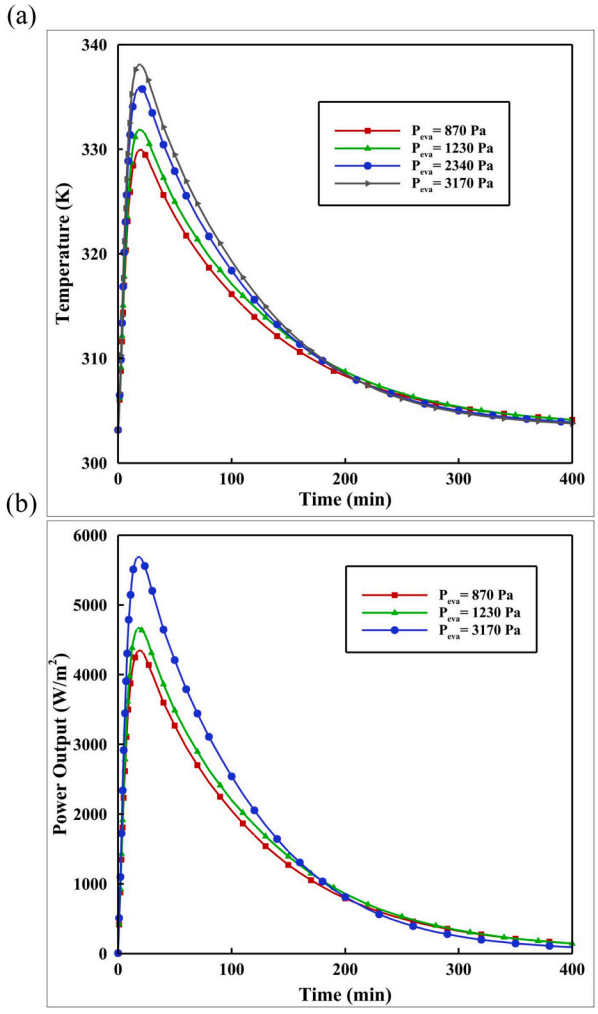

Fig. 16. Variation of (a) temperature and (b) output power for different evaporator pressures.

calculated based on Eq. (16) and defined to be 69.2 %, 65.5 %, and 37.7 % for the optimum Y-shaped fin, straight fin, and no fin cases, respectively. The efficiency of the adsorption cycle, based on Eq. (17), has been also calculated to be 75.3 %, 57.2 %, and 42.7 % for the optimum Y-shaped fin, straight fin, and no fin cases, respectively.

6. Conclusions

In the current study, the transient coupled heat and mass transfer in a zeolite bed containing straight and Y-shaped fins have been modeled, aiming to overcome the limitation of heat transfer in the bed. A parametric study is performed to study the influence of fin geometrical parameters, length, and branch angles, on the adsorption process performance. The average outlet temperature of HTF has been considered as the criterion, and the optimized geometry of the fin has been defined by applying RSM analysis. Based on this analysis, the effect of fin length is much higher than the angle between the branches. For the optimal design, an increase of 4.6 K and 8.7 K in the average outlet temperature is observed compared to the case with a straight fin and the case without fin, respectively. The average output power of 2265.4 W/m^2 is calculated for the optimum design, which shows 103 % and 238.8 % improvement compared to the case with straight fins and without fin, respectively. The optimized case with 6 fins has been taken into consideration and the influence of different parameters such as evaporator pressure and fin numbers has been investigated in the optimized case considering the output power, water uptake, and HTF outlet temperature. Based on the results, the power output and HTF outlet temperature enhance significantly with the increase of evaporator pressure, as a result of augmenting water uptake. The effect of fin numbers has been also studied and the best performance has been observed for the case with 8 fins. Investigating the performance of the system in two different designs without fins and including Y-shaped fins during the desorption process reveals a significant increase in bed temperature by adding optimized Y-shaped fins. The average temperature in the zeolite bed is reported to be 345 K in the case without fins and 396 K in the optimum case. The efficiency of the reactor for the optimum design has been defined as 69.2 and 75.3 % for the desorption and adsorption processes, respectively.

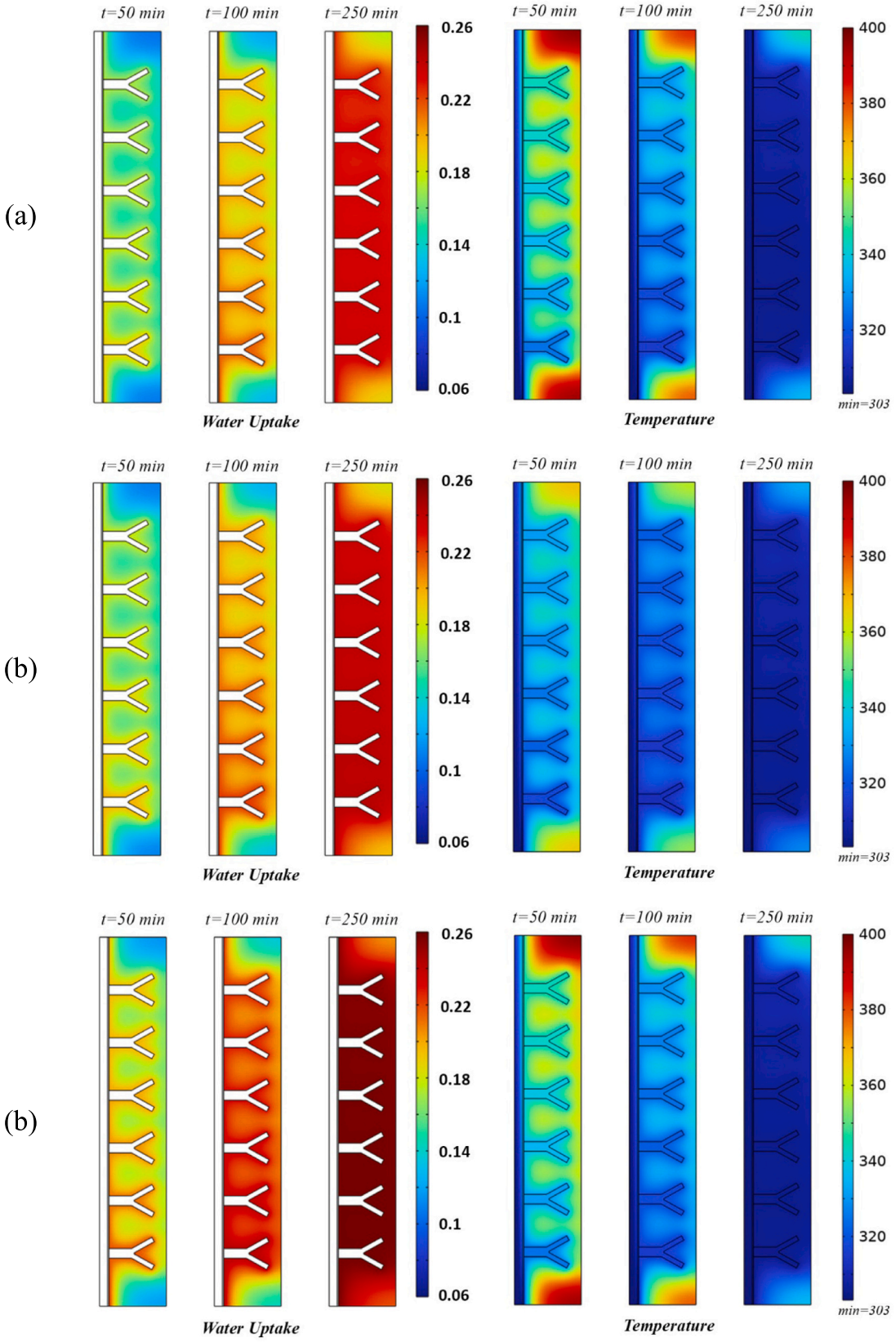

Fig. 17. Variation of temperature and water uptake at 50, 100, and 250 min for the optimized case at P_{evap} = (a) 873.35 Pa, (b) 1230 Pa, and (c) 3170 Pa.

Table 5
Parameters used for the desorption process model

Parameter	Value	Unit	Description
P_{Con}	4247	Pa	Condenser pressure
T_{init}	303.15	K	Initial temperature
T_{hot}	453	K	Hot HTF inlet temperature

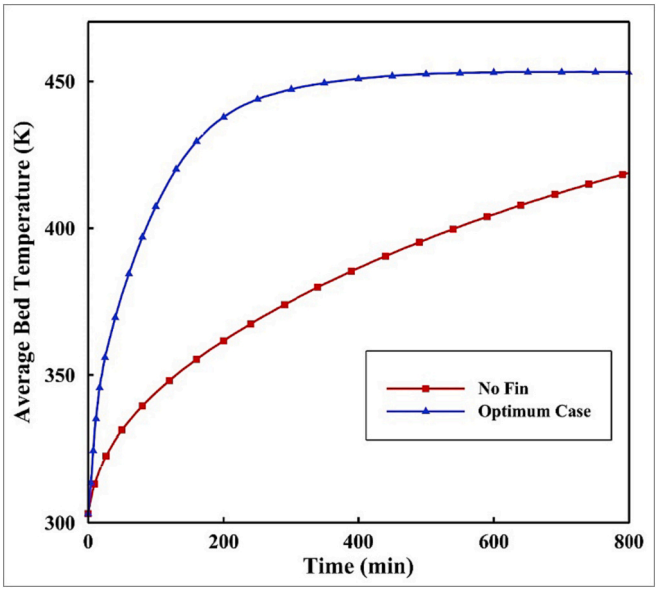

Fig. 18. The variation of bed temperature for the optimum case and the case without fin during the desorption process

CRediT authorship contribution statement

Elham Abohamzeh: Conceptualization, Data curation, Investigation, Methodology, Software, Validation, Visualization, Writing – original draft, Writing – review & editing. **Seyed Ehsan Hosseinizadeh:** Conceptualization, Investigation, Methodology, Software, Validation, Visualization. **Georg Frey:** Conceptualization, Investigation, Methodology, Project administration, Resources, Supervision, Writing – original draft, Writing – review & editing.

Declaration of competing interest

The authors declare that they have no known competing financial interests or personal relationships that could have appeared to influence the work reported in this paper.

Data availability

Data will be made available on request.

References

[1] P. Huovila, M. Ala-Juusela, L. Melchert, S. Pouffary, C.-C. Cheng, D. Ürge-Vorsatz, S. Koeppel, N. Svenningsen, P. Graham, Buildings and Climate Change: Summary for Decision-Makers, 2009.
[2] L. Pérez-Lombard, J. Ortiz, C. Pout, A review on buildings energy consumption information, Energ. Buildings 40 (3) (2008) 394–398.
[3] G. Energy, CO2 Status Report, IEA (International Energy Agency), Paris, France, 2019.
[4] T.R.S. Gbenou, A. Fopah-Lele, K. Wang, Recent status and prospects on thermochemical heat storage processes and applications, Entropy 23 (8) (2021) 953.
[5] R. Bravo, C. Ortiz, R. Chacartegui, D. Friedrich, Hybrid solar power plant with thermochemical energy storage: a multi-objective operational optimisation, Energ. Conver. Manage. 205 (2020) 112421.
[6] U. Tesio, E. Guelpa, C. Ortiz, R. Chacartegui, V. Verda, Optimized synthesis/design of the carbonator side for direct integration of thermochemical energy storage in small size concentrated solar power, Energy Conversion and Management: X 4 (2019) 100025.
[7] L. Scapino, C. De Servi, H.A. Zondag, J. Diriken, C.C.M. Rindt, A. Sciacovelli, Techno-economic optimization of an energy system with sorption thermal energy storage in different energy markets, Appl. Energy 258 (2020) 114063.
[8] A. Çağlar, The effect of fin design parameters on the heat transfer enhancement in the adsorbent bed of a thermal wave cycle, Appl. Therm. Eng. 104 (2016) 386–393.
[9] S. Mitra, M. Muttakin, K. Thu, B.B. Saha, Study on the influence of adsorbent particle size and heat exchanger aspect ratio on dynamic adsorption characteristics, Appl. Therm. Eng. 133 (2018) 764–773.
[10] K. Kant, A. Shukla, D.M.J. Smeulders, C.C.M. Rindt, Analysis and optimization of the closed-adsorption heat storage bed performance, J. Energy Storage 32 (2020) 101896.
[11] B. Golparvar, H. Niazmand, A. Sharafian, A.A. Hosseini, Optimum fin spacing of finned tube adsorber bed heat exchangers in an exhaust gas-driven adsorption cooling system, Appl. Energy 232 (2018) 504–516.
[12] K. Kant, R. Pitchumani, Analysis of a novel constructal fin tree embedded thermochemical energy storage for buildings applications, Energ. Conver. Manage. 258 (2022) 115542.
[13] C. Reichl, D. Lager, G. Englmair, B. Zettl, M. Popovac, Fluid dynamics simulations for an open-sorption heat storage drum reactor based on thermophysical kinetics and experimental observations, Appl. Therm. Eng. 107 (2016) 994–1007.
[14] A. Kurniawan, A. Rachmat, CFD Simulation of Silica Gel as an Adsorbent on Finned Tube Adsorbent Bed, EDP Sciences, p. 01014.
[15] A. Crespo, A. Frazzica, C. Fernández, Á. de Gracia, Optimizing the discharge process of a seasonal sorption storage system by means of design and control approach, Journal of Energy Storage 60 (2023) 106652.
[16] R.H. Mohammed, O. Mesalhy, M.L. Elsayed, L.C. Chow, Performance evaluation of a new modular packed bed for adsorption cooling systems, Appl. Therm. Eng. 136 (2018) 293–300.
[17] R. Salgado-Pizarro, A. Calderón, A. Svobodova-Sedlackova, A.I. Fernández, C. Barreneche, The relevance of thermochemical energy storage in the last two decades: the analysis of research evolution, J. Energy Storage 51 (2022) 104377.
[18] B. Mette, Experimentelle und numerische Untersuchungen zur Reaktionsführung thermochemischer Energiespeicher, 2014.
[19] P. Tatsidjodoung, N. Le Pierrès, L. Luo, A review of potential materials for thermal energy storage in building applications, Renew. Sustain. Energy Rev. 18 (2013) 327–349.
[20] X. Zheng, T.S. Ge, R.Z. Wang, Recent progress on desiccant materials for solid desiccant cooling systems, Energy 74 (2014) 280–294.
[21] D. Jähnig, R. Hausner, W. Wagner, C. Isaksson, Thermo-Chemical Storage for Solar Space Heating in a Single-Family House, Proceeding of Ecostock, New Jersey, 2006.
[22] A.A. Askalany, M. Salem, I.M. Ismail, A.H.H. Ali, M.G. Morsy, A review on adsorption cooling systems with adsorbent carbon, Renew. Sustain. Energy Rev. 16 (1) (2012) 493–500.
[23] L. Scapino, H.A. Zondag, J. Van Bael, J. Diriken, C.C.M. Rindt, Sorption heat storage for long-term low-temperature applications: a review on the advancements at material and prototype scale, Appl. Energy 190 (2017) 920–948.
[24] B.H. Thomas Herzog, Jochen Jänchen, Udo Hellwig, New innovative molecular sieves in energy engineering, 25. Deutsche Zeolith-Tagung, Hamburg, Germany.
[25] A.I. Khuri, S. Mukhopadhyay, Response surface methodology, Wiley Interdisciplinary Reviews: Computational Statistics 2 (2) (2010) 128–149.
[26] C. Liu, H. Yang, Multi-objective optimization of a concrete thermal energy storage system based on response surface methodology, Appl. Therm. Eng. 202 (2022) 117847.
[27] F. Ahmed, M.S. Abdul Aziz, M.R.R. Mohd Arif Zainol, K.C. Yee, F. Shaik, D.S. Che Halin, M.A.A. Mohd Salleh, M. Kheimi, Design, modelling and optimization of a novel concentrated solar powered (CSP) flash desalination system involving direct heating and pressure modulation using response surface methodology (RSM), Sustainability 14 (18) (2022) 11558.
[28] L. Sun, C.-L. Zhang, Evaluation of elliptical finned-tube heat exchanger performance using CFD and response surface methodology, Int. J. Therm. Sci. 75 (2014) 45–53.
[29] H. Alshihmani, M.-J. Maghrebi, M. Sardarabadi, Thermal performance prediction of a phase change material based heat-sink cooling system for a printed circuit board, using response surface method, J. Energy Storage 55 (2022) 105499.
[30] R.-J. Clark, A. Mehrabadi, M. Farid, State of the art on salt hydrate thermochemical energy storage systems for use in building applications, J. Energy Storage 27 (2020) 101145.
[31] A. Çağlar, Design and Experimental Testing of an Adsorbent Bed for a Thermal Wave Adsorption Cooling Cycle, 2012.
[32] İ. Solmuş, An Experimental Study on the Performance of an Adsorption Cooling System and the Numerical Analysis of its Adsorbent Bed, 2011.
[33] F.W. John Thomas, B. Crittenden, Adsorption Technology and Design, Butterworth-Heinemann, 1998.
[34] E. Glueckauf, Theory of chromatography. Part 10.—Formulæ for diffusion into spheres and their application to chromatography, Trans. Faraday Soc. 51 (1955) 1540–1551.
[35] B.P. Bering, M.M. Dubinin, V.V. Serpinsky, Theory of volume filling for vapor adsorption, J. Colloid Interface Sci. 21 (4) (1966) 378–393.
[36] R.E. Critoph, H.L. Turner, Performance of Ammonia-Activated Carbon and Ammonia Zeolite Heat Pump Adsorption Cycles, pp. 202–11.

[37] İ. Solmuş, C. Yamalı, B. Kaftanoğlu, D. Baker, A. Çağlar, Adsorption properties of a natural zeolite–water pair for use in adsorption cooling cycles, Appl. Energy 87 (6) (2010) 2062–2067.
[38] L.W. Wang, R.Z. Wang, R.G. Oliveira, A review on adsorption working pairs for refrigeration, Renew. Sustain. Energy Rev. 13 (3) (2009) 518–534.
[39] C. Latrille, A. Zoia, Estimating apparent diffusion coefficient and tortuosity in packed sand columns by tracers experiments, J. Porous Media 14 (6) (2011).
[40] M.J. MacDonald, C.F. Chu, P.P. Guilloit, K.M. Ng, A generalized Blake-Kozeny equation for multisized spherical particles, AICHE J. 37 (10) (1991) 1583–1588.
[41] A.D. Vdi-Wärmeatlas, 23: Wärmeleitfähigkeit der Flüssigkeiten in W/mK. 7. erweiterte Auflage, VDI-Verlag, Düsseldorf, 1994.
[42] L.M. Sun, N.B. Amar, F. Meunier, Numerical study on coupled heat and mass transfers in an absorber with external fluid heating, Heat Recovery Systems and CHP 15 (1) (1995) 19–29.
[43] M.W. Ellis, An Evaluation of the Effect of Adsorbent Properties on the Performance of a Solid Sorption Heat Pump, Georgia Institute of Technology, 1996.
[44] A. Çağlar, C. Yamalı, D.K. Baker, Two dimensional transient coupled analysis of a finned tube adsorbent bed for a thermal wave cycle, Int. J. Therm. Sci. 73 (2013) 58–68.
[45] F.P. Incropera, D.P. DeWitt, T.L. Bergman, A.S. Lavine, Fundamentals of Heat and Mass Transfer, Wiley, New York, 1996.
[46] A. Coppedè, S. Gaggero, G. Vernengo, D. Villa, Hydrodynamic shape optimization by high fidelity CFD solver and Gaussian process based response surface method, Appl. Ocean Res. 90 (2019) 101841.
[47] H. Jahangir, J.A. Esfahani, M. Pourali, K.C. Kim, Parameter study of a porous solar-based propane steam reformer using computational fluid dynamics and response surface methodology, Int. J. Hydrogen Energy 47 (86) (2022) 36465–36481.
[48] J.W. Wu, M.J. Biggs, E.J. Hu, Dynamic model for the optimisation of adsorption-based desalination processes, Appl. Therm. Eng. 66 (1–2) (2014) 464–473.
[49] M. Abou Elfadil, Investigations and Technical Development of Adsorption Thermal Energy Storage Systems with Simulation and Different Control Strategies, 2021.